Cold-working effect on magnetic properties in the Heusler alloys

Kôki Ikeda and Seiki Takahashi
Faculty of Engineering, Iwate University, Morioka 020, Japan
(Received 2 April 1984)

The cold-working effect on the average magnetic interaction ($\bar{J}$), the spontaneous magnetization at 0 K (M_0), and the magnetic transition temperature (Θ_m) in the Heusler alloys is formulated by means of dislocation theory with consideration of ferromagnetic and antiferromagnetic interactions between Mn atoms. The Mn atoms near the antiphase boundaries produced by plastic deformation have a different atomic environment (i.e., a different $\bar{J}$ value) from that in the normal state and cause a marked effect of cold working on the magnetic properties. The numerical estimation is given for two ferromagnetic Heusler alloys, Pd_2MnSn and Ni_2MnSn. A remarkable reduction of M_0 in the plastically deformed Pd_2MnSn, which was experimentally observed by previous investigators, is interpreted in the light of the present calculated results.

I. INTRODUCTION

The magnetic interaction between the localized magnetic moments in a metallic system has been of considerable interest experimentally and theoretically for over a decade. The Heusler alloy with a chemical formula X_2MnY, where X is an element of the Co, Ni, and Cu families and Y is an element of the group-IIIb, -IVb, and -Vb families, is a suitable material for such a study.[1] Namely, the Mn atom has a localized magnetic moment of about $4\mu_B$, whereas no definite magnetic moment is observed on the other component atoms except for the alloys containing Co.[2] Because Mn atoms are widely separated by nonmagnetic Y atoms, the Mn atoms have been considered to be coupled via conduction electrons by the s-d interaction of the Ruderman-Kittel-Kasuya-Yosida type,[3] or that of the double-resonance type by Caroli and Blandin.[4,5]

The calculation based on the latter model for the ferromagnetic Cu_2MnY has given a negative Curie temperature.[6] The investigation of the Mn-Mn interactions in ferromagnetic Pd_2MnSn ($T_c=189$ K) and Ni_2MnSn ($T_c=344$ K) by neutron-spin-wave scattering[7] has uncovered the ferromagnetic coupling between Mn atoms at a short-range distance. Namely, the exchange constants at long distances have an oscillatory character and validate the prediction by the s-d interaction based on the nearly-free-electron model,[3] but the positive sign of Mn-Mn coupling constants at the third- and sixth-nearest-neighbor (where NN denotes nearest neighbor) distances are the opposite of those expected from this model. Concerning this short-range ferromagnetic coupling between Mn atoms, an improvement has been made in the calculation by the d-resonance model.[8–10] On the other hand, Kasuya[11] has proposed an explanation in terms of the virtual double-exchange interaction where the electronic state of X atoms plays an important role.

Shinohara *et al.*[12] have recently found a remarkable reduction of the magnetization by plastic deformation and a recovery of this reduction by heat treatment (partly by the 300 °C annealing and completely by the 800 °C annealing) in Pd_2MnSn. Schaf *et al.*[13] later found that some additional NMR signals containing the reduction of the antiferromagnetic Mn-Mn coupling at the second-NN distance[14] appear in the deformed Pd_2MnSn alloy. The experimental results by Shinohara *et al.*[12] have been successfully explained[15] by means of the modified slip-induced directional-order model[16,17] with consideration of ferromagnetic and antiferromagnetic interactions between Mn atoms. According to this model, the number of Mn atoms at the "irregular" sites near the antiphase boundary (APB), which is produced by plastic deformation, is proportional to the dislocation density at the early stage of plastic deformation and to its square root at the advanced stage.

The magnetic interactions between Mn atoms at the regular sites have been discussed in connection with their electron concentration and lattice dimension. However, the Mn-Mn interactions at the first- and second-NN distances, which appear in deformed alloys, are considered to be far stronger than the interaction between Mn atoms at regular sites. Thus, the cold-working, as well as the atomic disordering or the composition discrepancy from stoichiometry, changes the magnetic properties. The investigation of the correlation of the magnetic properties and dislocations is a new method for studying the magnetic interactions at short distances. If the information on this correlation is elucidated, one might, conversely, investigate the superlattice dislocations from the magnetic measurements.

In this work the magnetic interactions, magnetization, and magnetic transition temperature in the cold-worked Heusler alloys, except Co_2MnY, are formulated by application of the modified slip-induced directional-order model. On the basis of the experimental values of Mn-Mn interactions,[7,14] the numerical estimation is given for Pd_2MnSn and Ni_2MnSn. Lastly, the experimental results in Pd_2MnSn by Shinohara *et al.*[12] are analyzed in comparison with these calculated results, and the cause of an anomalous reduction in the magnetization of crushed Pd_2MnSn alloys is discussed.

II. CRYSTAL STRUCTURE AND PLASTIC DEFORMATION

In the $L2_1$-type structure of the Heusler alloy, X atoms occupy the corner sites of the bcc lattice, i.e., A and C sites, while Mn and Y atoms occupy alternate body-centered sites, i.e., B and D sites, respectively (see Fig. 1). Two kinds of APB's may be considered in this superlattice. Namely, the APB's which have the displacements of $(a_0/4)\langle 111\rangle$ or $(a_0/2)\langle 100\rangle$ between both sides of the APB's, are denoted APB(1) and APB(2), respectively. Here, a_0 is the lattice parameter. Dislocations nucleate by applying external stress. The dislocations, whose Burgers vector is $(a_0/4)\langle 111\rangle$, slip over the $\{110\}$ glide planes. These superlattice dislocations are accompanied by APB's over the $\{110\}$ glide planes. The first dislocation creates ABP(1) over the $\{110\}$ glide plane, the next creates APB(2) over the $\{110\}$ glide plane, the third again creates APB(1) over this glide plane, and the fourth makes the glide plane recover. Thus, Mn atoms occupy the first and second NN's of the regular Mn site across APB(1) and APB(2), respectively.

The area of APB(i), induced by plastic deformation, is given by

$$A_i = \int_v l_i ds \ , \tag{1}$$

where l_i is the spacing between two dislocations composing APB(i). l_i takes a constant value deduced from the sum of the APB energy and the elastic interaction energy between individual dislocations constituting superlattice dislocations. ds is a segment of one of these dislocations. The integral is performed over the entire specimen. The area A_i per unit volume is rewritten as $A_1=\bar{l}_1\rho/2$ or $A_2=\bar{l}_2\rho/4$, where ρ is the dislocation density defined as the whole dislocation length per unit volume. Thus, the appearance ratio of the irregular Mn atoms at X and/or Y sites by plastic deformation is given by

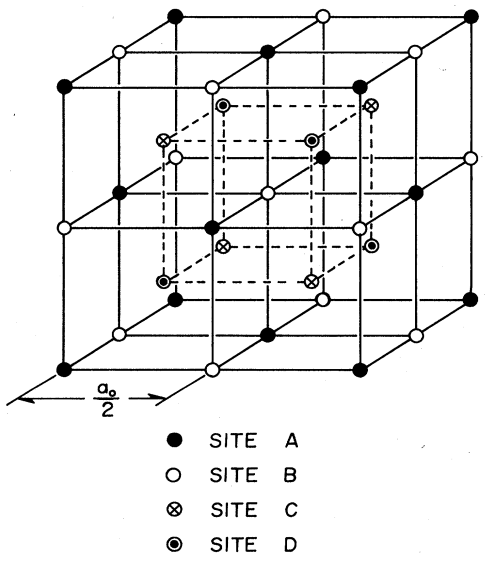

FIG. 1. Atomic arrangement of the Heusler ($L2_1$-type) structure.

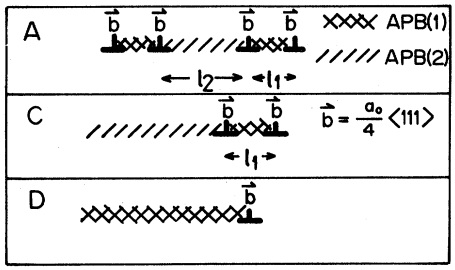

FIG. 2. Superlattice dislocation configurations of the Heusler ($L2_1$-type) alloy after Leamy *et al.* (Ref. 18). The notation A, C, and D is employed to describe three types of superlattice dislocations.

$$P_i=(S^2a_0/\sqrt{2})A_i \ , \tag{2}$$

where S is the long-range-order parameter in the specimen before plastic deformation.

According to Takahashi and Shinohara,[15] there are possibly three types of superlattice dislocations in the $L2_1$-type structure; in the first type, four dislocations make a bundle, the next type distributes, making a pair, and the last distributes independently and free from the attractive force of APB's. They are called A-, C-, and D-type superlattice dislocations, respectively, after the case of the $D0_3$-type Fe_3Al alloy[18] (see Fig. 2). When the energy of APB(2) is larger than that of APB(1), the A-type dislocations nucleate by the external stress.[18] At the early stage of plastic deformation, where the A-type dislocation may be the main distributor, the appearance ratios of Mn atoms at X and Y sites are, respectively, given by

$$P_1^A=(S^2a_0\bar{l}_1/2\sqrt{2})\rho \ , \tag{3}$$

$$P_2^A=(S^2a_0\bar{l}_2/4\sqrt{2})\rho \ . \tag{4}$$

The $\bar{l}_1$ value takes a constant value in the C-type superlattice dislocations. On the other hand, $\bar{l}_i$ is a function of the dislocation density and its distribution at the advanced stage. If the D-type superlattice dislocations are homogeneously distributed, $\bar{l}_i \propto 1/\sqrt{\rho}$. Thus, the ratios for the C- and D-type superlattice dislocations are, respectively, obtained as follows:

$$P_1^C=(S^2a_0\bar{l}_1/2\sqrt{2})\rho \ , \tag{5}$$

$$P_2^C=(S^2a_0/2\sqrt{2})\sqrt{\rho} \ , \tag{6}$$

$$P_1^D=S^2a_0\sqrt{\rho} \ , \tag{7}$$

$$P_2^D=(S^2a_0/2)\sqrt{\rho} \ . \tag{8}$$

III. INFLUENCE OF COLD WORKING ON MAGNETIC INTERACTION

In the cold-worked Heusler alloys the Mn atoms at irregular sites appear along the $\{110\}$ APB. These Mn atoms have a different atomic environment from that in the normal state, as shown in Figs. 3(a) and 3(b). The 0, I, II, and III planes are the $\{110\}$ planes at the distances of $\sqrt{2}(2k+1)a_0/8$ ($k=0$, 1, 2, and 3, respectively) from APB. Table I shows the numbers of Mn-Mn pairs at each

TABLE I. Number of neighboring Mn atoms around the host Mn atoms at the jth-nearest-neighbor distance r_j in the normal state, and on the 0, I, II, and III planes very close to APB(1) and APB(2) in the Heusler ($L2_1$-type) alloys and the $B2$- and $A2$-type alloys.

jth nearest-neighbor sites				1	2	3	4	5	6	7	8	9	10	11	12	13	14	15	16	17
$(4r_j/a_0)^2$				3	4	8	11	12	16	19	20	24	27	32	35	36	40	43	44	48
Total number of atom pairs				8	6	12	24	8	6	24	24	24	32	12	48	30	24	24	24	8
z_j	$L2_1$-type structure	Normal state		0	0	12	0	0	6	0	0	24	0	12	0	0	24	0	0	8
		APB(1)	0 plane	1	0	7	5	0	4	5	0	14	6	7	12	0	12	5	0	6
			I plane	0	0	11	2	0	4	3	0	18	5	7	8	0	16	3	0	6
			II plane	0	0	12	0	0	6	1	0	20	3	11	4	0	16	3	0	6
			III plane	0	0	12	0	0	6	0	0	24	0	11	2	0	22	2	0	6
		APB(2)	0 plane	0	2	7	0	2	4	0	12	14	0	7	0	12	12	0	10	6
			I plane	0	0	11	0	2	4	0	6	18	0	7	0	8	16	0	10	6
			II plane	0	0	12	0	0	6	0	2	20	0	11	0	8	18	0	4	6
			III plane	0	0	12	0	0	6	0	0	24	0	11	0	2	22	0	4	6
	B2-type structure			0	3	6	0	4	3	0	12	12	0	6	0	15	12	0	12	4
	A2-type structure			2	3/2	3	6	2	3/2	6	6	6	8	3	12	15/2	6	6	6	2

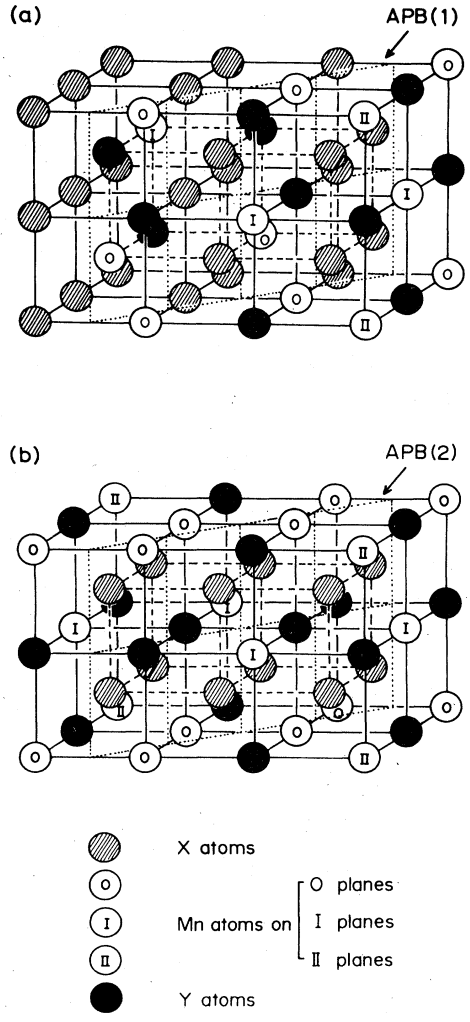

FIG. 3. Atomic arrangements of the Heusler ($L2_1$-type) structure after the (a) $(a_0/4)\langle 111\rangle$ and (b) $(a_0/2)\langle 111\rangle$ dislocations have slipped over the $\{110\}$ glide plane and created APB(1) and APB(2), respectively.

NN distance for the host Mn atoms on the 0, I, II, and III planes. The Mn atoms near APB(2) exhibit an atomic disorder similar to the $B2$-type structure. The Mn-Mn pairs at the first-NN distance appear on the 0 planes near APB(1).

According to Noda and Ishikawa,[7] the magnetic interactions between Mn atoms at distances further than the ninth-nearest neighbor ($r \gtrsim 8$ Å) in the Heusler alloys Pd_2MnSn and Ni_2MnSn have an oscillatory character which is similar to the theoretical prediction of the simple s-d model. At short distances, however, Noda and Ishikawa found a large deviation from this theoretical prediction. From the NMR studies for the off-stoichiometric Heusler alloys, Le Dang *et al.*[14] have found that excess Mn atoms substituted onto Y sites form antiferromagnetic localized moments in the ferromagnetic hosts, and have estimated the Mn-Mn coupling constant with the second-NN distances as $J_2=-0.91$ and -0.47 meV for Pd_2MnSn and Ni_2MnSn, respectively, from the temperature dependence of hyperfine fields. Furthermore, the Mn-Mn interaction at the first-NN distance in the Heusler alloys has been considered to be antiferromagnetic on the basis of the analysis of the magnetic structures in Pd_2MnIn (Ref. 19) and Pd_2MnGe (Ref. 20).

Figure 4 shows the exchange interactions as a function of the Mn-Mn distance in Pd_2MnSn and Ni_2MnSn. These $J(r)$ curves are based on two experimental reports[7,14] and on the theoretical estimation of the direct exchange interaction for a pair of Mn atoms in Cu at the first-NN distance [$J(2.61$ Å$)=-8$ meV].[10] According to Noda and Ishikawa,[7] the magnetic interactions between Mn atoms as far as $r=\sqrt{3}a_0$ suffice to reproduce the observed T_c values for both alloys. If the exchange interactions between Mn atoms at further distances than $\sqrt{3}a_0$ are neglected, the average magnetic interaction in the Heusler alloys is given by

$$\bar{J}=\sum_{j=1}^{17} z_j J_j \ , \tag{9}$$

where z_j and $J_j=J(r_j)$ are the number and the coupling

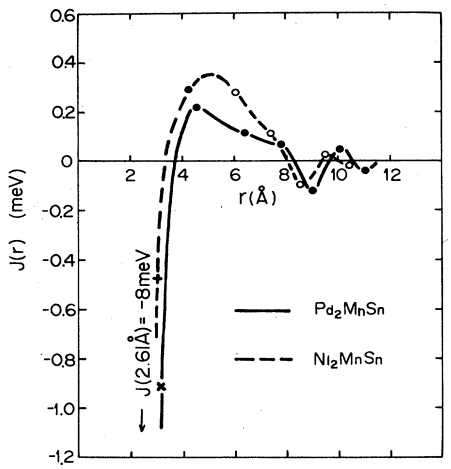

FIG. 4. Exchange interactions between Mn atoms in two ferromagnetic Heusler alloys, Pd_2MnSn and Ni_2MnSn, which were estimated experimentally by Noda and Ishikawa (Ref. 7) (● and ○) and by Le Dang *et al.* (Ref. 14) (× and +), and theoretically by Malmström *et al.* (Ref. 10) [$J(2.61\ \text{Å})=-8$ meV].

constant of the Mn-Mn pairs at the jth-nearest-neighbor distance (r_j), respectively. The z_j values are shown in Table I for each Mn atom in the normal state and on the 0, I, II, and III planes near APB(1) and APB(2).

The magnetic interactions of the Mn atoms at irregular sites near APB's are calculated by using the experimental $J(r)$ curves for both Heusler alloys in Fig. 4. Table II shows the calculated results of the magnetic interactions for irregular Mn atoms near APB's, along with those for the Mn atoms in the normal state, $J(N)$. Here, $J(i\text{-}0)$, $J(i\text{-I})$, $J(i\text{-II})$, and $J(i\text{-III})$ are the values for the Mn atoms on the 0, I, II, and III planes near APB(i). As shown in Table II, only $J(1\text{-}0)$ is negative in both alloys, but $J(2\text{-}0)/J(N)$ is small, especially in Pd_2MnSn. The calculated results also show that the magnetic interaction,

TABLE II. Magnetic interactions on the Mn atoms in the normal state and on the 0, I, II, and III planes near APB(1) and APB(2) in Pd_2MnSn and Ni_2MnSn, calculated from the experimental $J(r)$ curves with an accuracy of 10% (see Fig. 4). Units are meV, except for the $J(i)/J(N)$ values (in %).

Magnetic interaction	Pd_2MnSn	Ni_2MnSn
$J(N)$	4.16	7.18
$J(1\text{-}0)$	−2.97	−1.35
$J(1\text{-I})$	3.92	6.93
$J(1\text{-II})$	3.67	6.72
$J(1\text{-III})$	4.19	7.12
$J(2\text{-}0)$	1.67	5.58
$J(2\text{-I})$	4.34	7.36
$J(2\text{-II})$	3.89	6.66
$J(2\text{-III})$	4.23	7.15
$\Delta J(1)/J(N)$	−1.88	−1.30
$\Delta J(2)/J(N)$	−0.61	−0.28

even at a short distance from an APB (e.g., on the I, II, and III planes), is the same as $J(N)$ within +12% and ±7% deviation for Pd_2MnSn and Ni_2MnSn, respectively. This suggests that the influence of plastic deformation on the Mn-Mn interactions is restricted within the Mn atoms very close to an APB.

IV. MAGNETIZATION AND MAGNETIC TRANSITION TEMPERATURE IN DEFORMED ALLOYS

The change of magnetic interactions between Mn atoms must have an influence on the magnetization and the magnetic transition temperature. According to the preceding section, on the planes along the APB which were produced by plastic deformation, especially on the 0 planes, the Mn atoms have a different $\bar{J}$ value from that in the normal state. The magnetic moments of these Mn atoms near an APB may therefore be different from those of the normal state, in magnitude and/or direction. The influence of cold working on the magnetization and the magnetic transition temperature is formulated in this section. $S=1$ is assumed for simplicity.

The net value of the saturation magnetization at 0 K in the plastically deformed Heusler alloys, M_0, can be written as

$$M_0=(N_0-N)\vec{\mu}_{\text{Mn}}+N\vec{\mu}'_{\text{Mn}}\ . \tag{10}$$

Here, N_0 is the total number of Mn atoms, $\vec{\mu}_{\text{Mn}}$ is the magnetic moment of the Mn atoms in the normal state, and N and $\vec{\mu}'_{\text{Mn}}$ are the number and the magnetic moment of the irregular Mn atoms near the APB, respectively. The variation rate of the spontaneous magnetization at 0 K is given by

$$\Delta M_0/M_0(N)=(N/N_0)(\alpha-1)\ , \tag{11}$$

where $M_0(N)=N_0\vec{\mu}_{\text{Mn}}$ and $\alpha=\vec{\mu}'_{\text{Mn}}/\vec{\mu}_{\text{Mn}}$. As can be seen from Table II, the Mn-Mn interaction on the 0 planes near APB(1), $J(1\text{-}0)$, is negative because of a negative and very strong value of J_1 (≈ -8 meV). If $\mu'_{\text{Mn}}=\mu_{\text{Mn}}$, i.e., $\alpha=-1$, Eq. (11) is determined only by the appearance ratio of irregular Mn atoms, N/N_0. Assuming that only $J(1\text{-}0)$ is negative, $\Delta M_0/M_0(N)=-2P_1$ [assumption (A)]. On the other hand, one obtains $\Delta M_0/M_0(N)=-2(P_1+P_2)$ if $J(1\text{-}0)$ and $J(2\text{-}0)$ are negative [assumption (B)].

The investigation of the atomic-environment effect on the magnetic moment of Mn atoms has been made in the disordered Ni-Mn alloys by the polarized-neutron diffuse scattering (Refs. 21 and 22) and NMR (Ref. 23) measurements. The results of these investigations suggest that the magnetic moment of isolated Mn atoms is parallel to the bulk Ni magnetization, whereas the Mn atoms with three or more Mn neighbors at the first-NN distance reduce or reverse their magnetic moments. Thus, the magnetic moments estimated by NMR experiments are $3.0\mu_B$, $2.5\mu_B$, and $-1.8\mu_B$ for isolated, reduced, and reversed Mn atoms, respectively.[23] If the Mn moments on the 0 and I planes near APB(1) and APB(2) become negligibly small, one obtains $\alpha=0$ and $N/N_0=2(P_1+P_2)$ [assumption (C)], which are the same results as of assumption (B). If

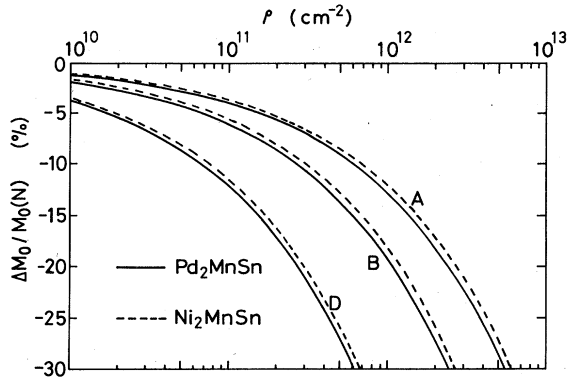

FIG. 5. Variation rate of the spontaneous magnetization at 0 K by plastic deformation, $\Delta M_0/M_0(N)$, as a function of the dislocation density ρ in Pd_2MnSn and Ni_2MnSn. Curves A, B, and D correspond to assumptions (A), (B), and (D), respectively.

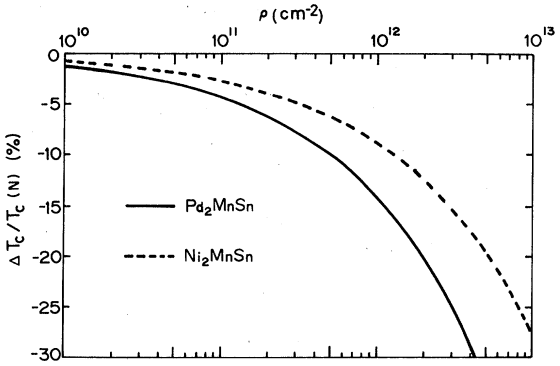

FIG. 6. Variation rate of the Curie temperature by plastic deformation, $\Delta T_c/T_c(N)$, as a function of the dislocation density ρ in Pd_2MnSn and Ni_2MnSn.

the influence of APB(1) and APB(2) extends to the III planes, $\Delta M_0/M_0(N)=-4(P_1+P_2)$ [assumption (D)].

Figure 5 shows $\Delta M_0/M_0(N)$ values in deformed Pd_2MnSn and Ni_2MnSn alloys which are calculated for assumptions (A)—(D) by Eqs. (7), (8), and (11) in the advanced stage of plastic deformation where the type-D superlattice dislocations are the main distributors. $\Delta M_0/M_0(N)$ is represented as a function of the dislocation density over the range 10^{10}—10^{13} cm^{-2}. Here, $a_0=6.380$ Å is adopted for Pd_2MnSn and $a_0=6.052$ Å is adopted for Ni_2MnSn (Ref. 1).

The change of Mn-Mn interactions by plastic deformation will also have an influence on the magnetic transition temperature. According to the molecular-field theory, the magnetic transition temperature Θ_m is given by

$$\Theta_m=\frac{2\bar{J}s(s+1)}{3k_B}\ . \tag{12}$$

Here, k_B is Boltzmann's constant and s is the localized spin. Assuming that the spin of these irregular Mn atoms is the same as that in the normal state, the influence of cold working on the magnetic transition temperature is determined only by the change of magnetic interactions according to Eq. (12).

According to the preceding section the variation rate of magnetic transition temperature by plastic deformation is written as

$$\frac{\Delta\Theta_m}{\Theta_m(N)}=\sum_{i=1}^{2}P_i[\Delta J(i)/J(N)]\ . \tag{13}$$

Here, $\Theta_m(N)$ is the magnetic transition temperature in the fully ordered alloy. The difference of magnetic interactions between the Mn atoms near APB(i) and in the normal state is expressed by

$$\Delta J(i)=\sum_{k=0,\mathrm{I},\mathrm{II},\mathrm{III}}[J(i-k)-J(N)]\ . \tag{14}$$

Table II also shows that $\Delta J(1)/J(N)$ and $\Delta J(2)/J(N)$ values are negative in both alloys, but are considerably stronger in the former alloy than in the latter.

In Fig. 6 the variation rate of the Curie temperature on plastic deformation for Pd_2MnSn and Ni_2MnSn is shown in the advanced stage of plastic deformation where the D-type superlattice dislocations are the main distributors. The variation rate is represented as a function of the dislocation density over the range 10^{10}—10^{13} cm^{-2}. This figure predicts the appearance of rapid lowering of T_c with plastic deformation advancing in both Heusler alloys (especially in Pd_2MnSn) as well as the case of M_0.

V. COMPARISON WITH EXPERIMENTAL RESULTS AND DISCUSSION

Shinohara *et al.*[12] have observed the remarkable reduction in the magnetization of Pd_2MnSn after the crushing treatment. Their experimental results are finally discussed on the basis of the present calculated results on M_0 and Θ_m. Table III is the summary of their results, where $\Delta C_m/C_m(N)$ is the variation rate of the Curie constant by cold working. The $\Delta\Theta_m/\Theta_m(N)$ and $\Delta C_m/C_m(N)$ values are estimated from the reversed susceptibility between 250 and 350 K. The estimation of the saturation magnetization is not easy for deformed Pd_2MnSn alloys, because the magnetization of the fully ordered alloy immediately satu-

TABLE III. Experimental results of the cold-working effect on some magnetic properties in the Pd_2MnSn alloy. Sample no. 1 is as-crushed and sample nos. 2 and 3 are annealed at 300 and 400 °C, respectively, for 10 h after crushing (Ref. 12).

Sample no.	$\Delta\Theta_m/\Theta_m(N)$ (%)	$\Delta C_m/C_m(N)$ (%)	$\Delta M_0^{\mathrm{I}}/M_0(N)$ (%)	$10^3\,\chi_{\mathrm{HF}}$ (emu/g-at.)	$\Delta M_0^{\mathrm{II}}/M_0(N)$ (%)
1	−8±1	−26±1	−59±1	9.3±0.4	−33±2
2	+1±1	−17±1	−43±1	11.8±0.4	−16±1
3			−21±1	4.3±0.4	−13±1

rates, whereas the cold working not only causes a reduction in the magnetization, but also induces a strong field dependence.

The field dependence of the magnetization in ferromagnets is generally represented by the H^{-2} term due to the rotation of magnetization and the H term originating in the induced magnetization by fields. In the M-versus-H curves of plastically deformed ferromagnets, it is known[24] that the H^{-1} term, which is associated with a local anisotropy, adds to these contributions. The M-versus-H curves of crushed Pd_2MnSn alloys are almost linear in fields higher than 2.6 T. As shown in Table III, however, the high-field susceptibility χ_{HF} in sample nos. 1 and 2 is larger by a factor of ~ 10 than that in disordered Ni-Mn alloys.[25]

The M_0 value in the crushed Pd_2MnSn was thus estimated in the following two ways from the high-field magnetization data at 4.2 K up to 9 T by Shinohara *et al.*[12] First, it was estimated from the extrapolation of the almost straight part in $H \geq 2.6$ T in the magnetization curves at $H \rightarrow 0$. Second, it was estimated from the extrapolation of the almost straight part in $H \geq 5.5$ T in the M-versus-H^{-1} plots as $H \rightarrow \infty$. The $\Delta M_0^{\mathrm{I}}/M_0(N)$ and $\Delta M_0^{\mathrm{II}}/M(N)$ values are estimated in the first and second ways, respectively.

Table III shows the following: (a) $\Delta C_m/C_m(N)$ in sample no. 2 is about two-thirds of that in sample no. 1, as well as the case of $\Delta M_0/M_0(N)$; (b) the ratio of $\Delta C_m/C_m(N)$ to $\Delta M_0^{\mathrm{I}}/M_0(N)$ is about 40% in sample nos. 1 and 2; (c) $\Delta M_0^{\mathrm{II}}/M_0(N)$ is similar to $\Delta C_m/C_m(N)$ in both samples. The Curie constant reflects the behavior of magnetic moments in the paramagnetic state. Moreover, $\Delta M_0^{\mathrm{I}}/M_0(N)$ and $\Delta M_0^{\mathrm{II}}/M_0(N)$ correspond to the variation rates of the saturation magnetization by plastic deformation at $H=0$ and ∞, respectively. The experimental facts suggest that after plastic deformation, in addition to the reversed Mn moments, the reduced Mn moments appear, and both are associated with the APB; the former disappears with increasing fields.

According to the calculated results of the preceding section, the dislocation density in crushed Pd_2MnSn alloys can be estimated from these experimental results. Figure 6 suggests that the dislocation density in the as-crushed sample (no. 1) is about 3.0×10^{11} cm^{-2}. $\Delta\Theta_m/\Theta_m(N)$ is -8% even in the as-crushed sample, whereas $\Delta M_0/M_0(N)$ and $\Delta C_m/C_m(N)$ show a much larger reduction than $\Delta\Theta_m/\Theta_m(N)$. This relatively small reduction of Θ_m concludes that the reduction of magnetic moments in this deformed alloy does not occur in all Mn atoms, but in the Mn atoms near the APB, because Θ_m is proportional to $s(s+1)$ [see Eq. (12)].

Lapworth and Jakubovics[26] have studied the magnetic properties of the Cu-Mn-Al Heusler alloys by Lorentz microscopy in relation to composition, heat treatment, and plastic deformation. They have observed that the magnetic domain wall (MDW) is pinned at the APB, which is induced not only thermally, but also by plastic deformation. This pinning is thought to be due to antiferromagnetic coupling between the Mn moments on both sides of the APB.

Thus the following model is proposed for the explanation of the large, negative values of $\Delta M_0/M_0(N)$ and $\Delta C_m/C_m(N)$ in Pd_2MnSn. A domain lying between both APB(1)'s with the width of R may be noticeable. The Mn moments couple antiferromagnetically along the APB and ferromagnetically in the domain. Figure 7 is a schematic explanation of the appearance of an antiferromagnetic domain. The Mn moments in the core of these domains with the narrow width ($R \leq R_c$) are unchanged in magnitude from those in outer wide domains, but are reversed in direction because of the negative J(1-0) value. Here, R_c is the critical width of the domain lying between APB(1)'s, which the ferromagnetic domain begins to invade.

In hard deformed crystals where the dislocation (namely, the APB also) distributes complicatedly, such domains of narrow width may be observable. The remarkable reduction of M_0 by cold working must be due not only to the considerable decrease of Mn moments near the APB, but also to the appearance of these antiferromagnetic domains. The MDW connecting the edges of both APB(1)'s, which is shown by the dotted lines in Fig. 7, moves with increasing fields. Thus, the magnetization is strongly induced by magnetic fields, but does not easily saturate because of the strong pinning at the APB. The significantly large value of $\Delta M_0^{\mathrm{I}}/M_0(N)$ and the rough agreement between $\Delta C_m/C_m(N)$ and $\Delta M_0^{\mathrm{II}}/M_0(N)$ are reasonably explained by this schematic.

According to the agreement between $\Delta C_m/C_m(N)$ and $\Delta M_0^{\mathrm{II}}/M_0(N)$, and to the remarkable reduction ($\sim 30\%$) of these values in the as-crushed sample, one may choose assumption (D) as a proper assumption for this alloy. Thus, curve D in Fig. 5 gives $\rho=6\times10^{11}$ cm^{-2} in sample no. 1. By the same analysis, moreover, $\rho=2\times10^{11}$ cm^{-2} is estimated for sample no. 2. These different values of ρ suggest that APB(1) preferentially disappears by the 300 °C annealing, i.e., the APB(1) energy is larger than the APB(2) energy. The significant decrease of χ_{HF} after the 400 °C annealing may show that APB(1) almost disappears by this heat treatment.

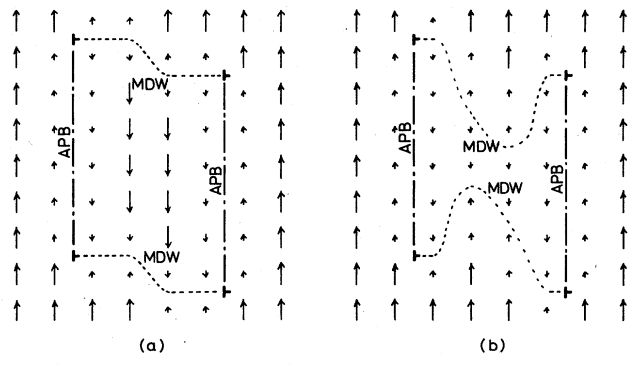

FIG. 7. Schematic explanation of the appearance of antiferromagnetic domains in the plastically deformed Pd_2MnSn alloys, which are associated with the domains lying between the APB(1) with narrow width ($R \leq R_c$). The volume of this antiferromagnetic domain decreases more in magnetic fields, (b), than in zero field, (a).

As the difference between both curves for Pd_2MnSn and Ni_2MnSn shows, a reduction of M_0 by cold working similar to that in Pd_2MnSn is expected in other Heusler alloys if the same assumption for the magnetic state of Mn atoms materializes. In the crushing treatment, similar experimental studies were made on Pd_2MnSn by means of measurements of magnetization[27] and Mössbauer effect.[28] The magnetization reduction was very small as compared to that of Pd_2MnSn, and the Mössbauer measurements revealed only two components of the dominant and weak spectra, which come from the Sb nuclei on the regular site and a defect site associated with the Heusler phase, respectively.

The remarkable reduction of M_0 by cold working in Pd_2MnSn, which suggests the disappearance of Mn moments as far as the III planes from APB and the appearance of the antiferromagnetic domains lying between APB's, may be anomalous. Not only does the antiferromagnetic interaction appear between the Mn atom very close to the APB, but the formation of magnetic moments of Mn atoms is also considered to be strongly influenced by the symmetry of atomic arrangement in addition to the numbers of neighboring Mn atoms. The narrow spacing between the APB, originating in the characteristic relation between the APB energy and the elastic interaction energy of dislocations, is probably preferred in this alloy.

This work has shown that the Mn atoms near the antiphase boundaries produced by plastic deformation have a different magnetic interaction value than that in the normal state and cause a marked effect on magnetic properties in the Heusler alloys. The influence of plastic deformation on the magnetic properties has been avoided by employing annealing as the complicated phenomenon, but by using the present formulation, it may be possible to study the magnetic interactions and magnetic moment distribution from a new point of view. The present results might also be useful for the estimation of the dislocation density and the study of its structure in a given specimen.

ACKNOWLEDGMENTS

One of us (K.I.) began this study in the Laboratoire de Physique des Solides, Université de Paris—Sud, and would like to thank Dr. M. T. Béal-Monod, Dr. P. Monod, and Dr. I. A. Campbell for their hospitality. Financial support from the Centre National de la Recherche Scientifique, France, is also acknowledged.

[1]P. J. Webster, Contemp. Phys. **10**, 559 (1969).
[2]P. J. Webster, J. Phys. Chem. Solids **32**, 1221 (1971).
[3]M. A. Ruderman and C. Kittel, Phys. Rev. **96**, 99 (1954); T. Kasuya, Prog,. Theor. Phys. **16**, 45 (1956); K. Yosida, Phys. Rev. **106**, 893 (1957).
[4]B. Caroli and A. Blandin, J. Phys. Chem. Solids **27**, 503 (1966).
[5]B. Caroli, J. Phys. Chem. Solids **28**, 1427 (1967).
[6]D. J. W. Geldart and P. Ganguly, Phys. Rev. B **1**, 3101 (1970).
[7]Y. Noda and Y. Ishikawa, J. Phys. Soc. Jpn. **40**, 690 (1976).
[8]P. Jena and D. J. W. Geldart, Phys. Rev. B **7**, 439 (1973).
[9]H. Alloul, J. Phys. F **4**, 1501 (1974).
[10]G. Malmström, D. J. W. Geldart, and C. Blomberg, J. Phys. F **6**, 233 (1976); **6**, 1953 (1976).
[11]T. Kasuya, Solid State Commun. **15**, 1119 (1974).
[12]T. Shinohara, K. Sasaki, H. Yamauchi, H. Watanabe, H. Sekizawa, and T. Okada, J. Phys. Soc. Jpn. **50**, 2904 (1981).
[13]J. Schaf, K. Le Dang, P. Veillt, and I. A. Campbell, J. Phys. F **13**, 1311 (1983).
[14]K. Le Dang, P. Veillt, and I. A. Campbell, J. Phys. F **8**, 1181 (1978).
[15]S. Takahashi and T. Shinohara, J. Phys. F **12**, 3115 (1982).
[16]S. Takahashi, Phys. Status Solidi B **52**, 141 (1972).
[17]S. Takahashi, Phys. Status Solidi A **42**, 201 (1977).
[18]H. J. Leamy, F. X. Kayer, and M. J. Marcinkowski, Philos. Mag. **20**, 763 (1969); **20**, 779 (1969).
[19]P. J. Webster and R. S. Tebble, Philos. Mag. **16**, 347 (1967).
[20]M. G. Natera, M. R. L. N. Murthy, R. J. Begum, and N. S. Satya Murthy, Phys. Status Solidi A **3**, 959 (1970).
[21]J. W. Cable and H. R. Child, J. Phys. (Paris) Colloq. **32**, C1-67 (1971).
[22]J. W. Cable and H. R. Child, Phys. Rev. B **10**, 4607 (1974).
[23]Y. Kitaoka, K. Ueno, and K. Asayama, J. Phys. Soc. Jpn. **44**, 142 (1978).
[24]S. Chikazumi, *Physics of Ferromagnetism* (Wiley, New York, 1964).
[25]K. Okuda, H. Mollymoto, and M. Date, J. Phys. Soc. Jpn. **47**, 1015 (1979).
[26]A. J. Lapworth and J. P. Jakubovics, Philos. Mag. **29**, 253 (1974).
[27]T. Shinohara and K. Sasaki (private communication).
[28]M. Blizzard and P. Boolchand, J. Appl. Phys. **50**, 2075 (1979).